33rd Annual International Conference of the IEEE EMBS
Boston, Massachusetts USA, August 30 - September 3, 2011

Electronic Performance of a Dual Inductive Link for a Wireless Neural Recording Implant

Alexander Rush, Student *Member, IEEE, EMBS*, Philip R. Troyk, *Senior Member, IEEE*

***Abstract*—This paper reports a dual inductive link to provide two-way wireless communication and power for a neural recording system. Particular emphasis is placed on explaining the challenges associated with two inductive links operating in the same space and possible solutions. This system uses a class E converter to sustain a large AC current in an external coil for transcutaneous energy transfer to an implant coil. A telemetry circuit generates a reverse-telemetry carrier frequency using an Integer-N PLL to support multiple outward data channels. Interference from the class E converter fundamental and harmonics is rejected using a differential coil configuration. An approach to filtering harmonic interference from the external power coil is also presented.**

I. Introduction

A wireless neural recording system requires power and forward data to be transferred to the implant. Power is typically transferred to the implant using a single inductive link, and forward data is transferred by modulating the power carrier. Reverse telemetry can be achieved by a method called load shift keying (LSK), whereby the impedance seen by the implanted power coil and resonating capacitor is changed either by shorting or opening the load, detuning the resonant tank, or changing the rectifier configuration. However, the data rate of reverse telemetry using this method is generally limited to a fraction of the power carrier frequency, which is typically in the low MHz range. To send raw data from 16 channels, which is our initial goal, assuming an ADC resolution of 10bits/sample and a sampling rate of 20kSamples/s, a reverse telemetry data rate of at least 3.2Mbps would be required.

Therefore, it is desirable to have another inductive link for reverse telemetry. For compactness these inductive links should operate in the same space, but to do so one must consider interactions between the power and data signals and coils. Various approaches have been proposed to minimize or mitigate interference between inductive links operating in the same space [1-3]. The design presented here uses new techniques as well as techniques similar to those presented in the literature and applies them to a dual inductive link for a wireless neural recording system.

For instance [2] presents an approach to maximize the difference between the constructive and destructive paths in a dual inductive link for the transfer of power and telemetry to a retinal prosthesis. This approach was applied to maximize the reverse telemetry signal for this design.

A differential antenna is commonly used for RFID applications as presented in [1]. This technique was used for the design presented, but primarily to cancel harmonic interference from the class E converter rather than to cancel interference at the power carrier frequency.

An approach to reducing harmonic interference from the power coil using low loss filters is also presented.

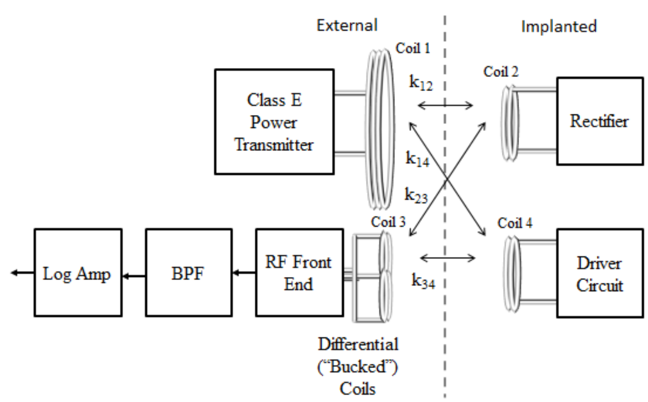

Figure 1. Dual inductive link for power and bidirectional data transfer system schematic.

Manuscript received April 15, 2011.
A. Rush is with the Illinois Institute of Technology, Chicago, IL 60616 USA (e-mail: rushale@iit.edu).
P. R. Troyk, is with Illinois Institute of Technology, Chicago, IL 60616 USA (e-mail: troyk@iit.edu).

II. System Implementation

Here we report a wireless power and bidirectional data transfer system implemented with a dual inductive link as illustrated in Fig. 1. A large AC current is generated in the external power coil using a class E converter. AC voltage is induced in the implanted power coil proportional to the coupling coefficient between the external and implanted power coils, k_{12}. This AC voltage is rectified to supply the chip with power and is used to generate a reference clock for the implant. The current in the external coil can also be FSK modulated at 1.25Mbps to send control data to the implant.

In the implant circuitry, the reference clock, derived from the 5MHz power carrier, is routed to an integer-N PLL to generate the reverse telemetry carrier, which is either ASK or BPSK modulated. Driver circuitry induces current in the implanted data coil, which is concentric to the implanted power coil, to generate the reverse telemetry signal.

Data is received by one of the external differential data coils with inductance L_3 and effective series resistance R_3. A differential coil configuration is often used in RFID receivers to cancel the large power signal at its fundamental frequency. However, for reverse telemetry, the RF front-end is not as limited in size as the implanted circuitry and a 3-pole high-pass filter (Coilcraft, Cary, IL) is sufficient to reject the interference from the power carrier. The main purpose of the differential antenna here is rejection of harmonics generated by the class E converter and falling within the frequency range of the reverse telemetry, as illustrated in Section IV, Differential Antenna.

For simplicity, reverse telemetry from the implant circuitry used ASK modulation and was demodulated with a bandpass filter and a log amp, as illustrated in Fig. 1.

III. CLASS E CONVERTER

The magnetic field for inductive powering was generated by a class-E converter operating at 5MHz. The coil which is external to the body and part of the class-E converter carried a current of 0.65A, had a radius of 3cm and 8 turns of litz wire.

Due to the large size of the power signal compared to the reverse telemetry signal, even small amounts of harmonic distortion, occurring at integer multiples of the power carrier frequency can obscure the reverse telemetry signal, which is at an integer multiple of the power carrier frequency.

Another source of interference can be the gate drive, which can couple to the external data coil from the gate-drain capacitance of the class E FET. Harmonics distortion resulting from normal operation of the class E converter and from the gate drive signal is illustrated in Fig. 2.

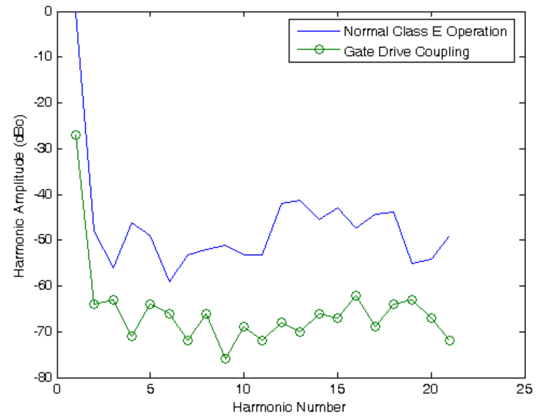

Figure 2. Class E harmonic interference during normal operation and from coupling of the gate drive signal into the series LC branch of the class E converter.

We have explored two different approaches to reduce harmonics in the external power coil. One way is to place a low pass filter in the series tank circuit as illustrated in Fig. 3a. The other approach, illustrated in Fig. 3b, is to place a notch filter in the series tank of the class E converter to attenuate the harmonic distortion at the reverse telemetry carrier frequency. For various reasons we chose to use a notch filter. Using this approach, the 12th harmonic (60MHz) which coincides with the reverse telemetry carrier, was attenuated by 15dB. In our initial work, we used a trimmer capacitor with a low Q (<5) at the reverse telemetry carrier frequency, 60MHz, and a higher Q is expected to improve performance.

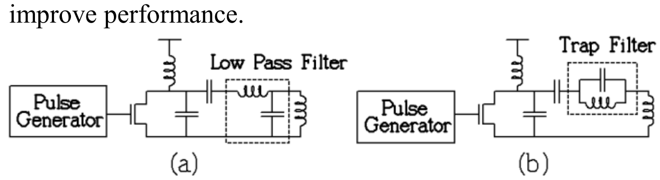

Figure 3. Methods of filtering class E harmonics from the series LC branch of the class E tank circuit.

IV. DIFFERENTIAL ANTENNA

The external data receiver antenna chosen was a pair of "bucked" coils with inner leads connected together and outer leads connected together and grounded. This has the effect of canceling both distant sources of RF magnetic interference as well as the power carrier which is presented almost equally to both of the bucked coils. The response to the implant data coil is maximal in the center of either of the bucked coils and very small at the edge of the bucked coils. The cancellation of harmonics generated by the class E converter, which fall in the frequency range of the reverse telemetry signal, is illustrated in Fig. 4.

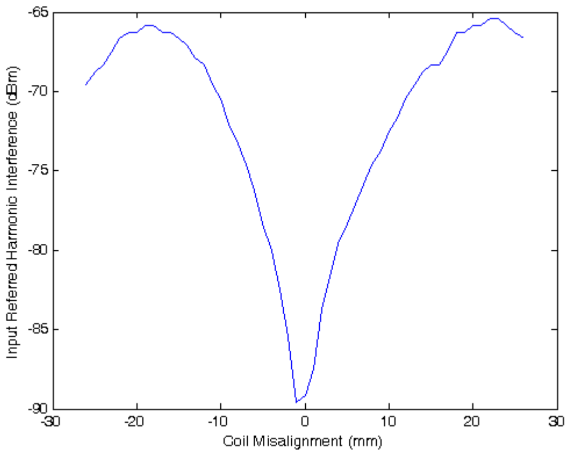

Figure 4. Illustration of harmonic interference nulling by differential antenna.

V. COILS PARAMETERS

In this section details of the dual inductive link, illustrated in Fig. 1, are given. In particular the physical dimension and inductances of the four coils are presented. The external and internal power coils are referred to as coil 1 and coil 2 respectively, and the external and internal data coils are referred to as coil 3 and coil4, respectively. Coil 3 refers specifically to one side of the external differential coil, since the implant data coil only couples strongly to the side with which it is coaxial.

Parameters of the power coils are given in Table I, and parameters of the data coils are given in Table II.

TABLE I. POWER COIL PARAMETERS

Parameters	**Coil 1**	**Parameters**	**Coil 2**
Inductance	4.62µH	Inductance	32.4µH
Length	9mm	Wire Diameter	25µm
Turns	7	Insulation Thickness	5µm
Radius	3cm	Radius	5mm
		Turns Per Layer	12
		Number of Layers	3

TABLE II. DATA COIL PARAMETERS

Parameters	**Coil 3**	**Parameters**	**Coil 4**
Inductance	55nH	Inductance	2.98µH
Length	15mm	Wire Diameter	25µm
Width	19mm	Insulation Thickness	5µm
Turns	1	Radius	4mm
Number of Layers	1	Turns Per Layer	12
		Number of Layers	1

Coil design was aided by an analytic model of the link, which space does not allow including here. The analytic model assesses the link performance given the coil physical parameters allowing the physical parameters to be iterated to find an optimal design. We found that the optimal ratio of implanted power and data coil radii for our design was close to 0.8.

In order to facilitate measurement of the dual coil link electrical parameters as well as to facilitate testing of the dual coil link performance we fabricated a coil form for winding the prototype concentric coplanar implant data coils.

The implant data coil and power coil were wound with 50AWG gold wire and wire bonded to a PCB for testing of electrical parameters and interfacing with the implant circuitry. Because inductance and coupling coefficient are determined by coil geometry, these parameters were measured at low frequency with a Solartron HP 1260 Impedance/Gain-Phase Analyzer.

VI. IMPLANT CIRCUITRY

The implant circuitry, illustrated in Fig. 5, generates a reverse-telemetry carrier frequency using an Integer-N PLL to support multiple outward data channels. The PLL design uses self-biasing techniques for supply rejection [5], has dimensions of 350um x 680um, and generates frequencies with a phase noise of -83dBc/Hz @100kHz offset, as measured at 80MHz.

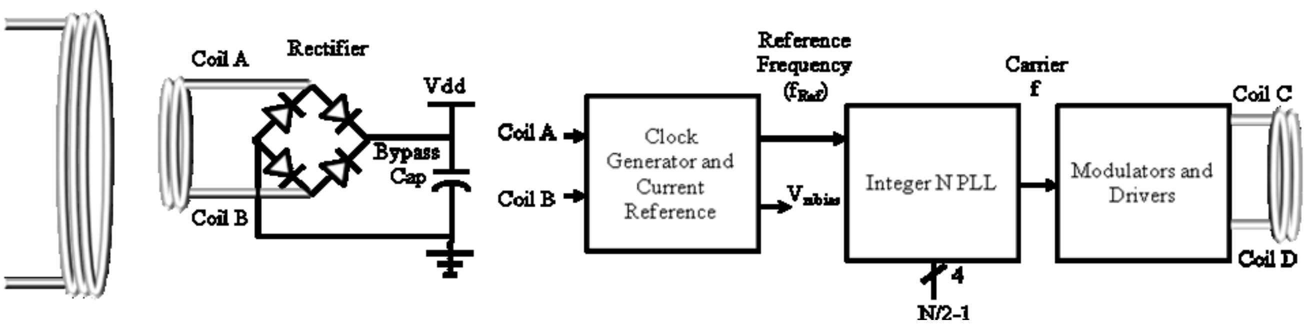

Figure 5. Schematic of Implanted Circuitry for Multi-Channel Wireless Neural Recording System (from [6])

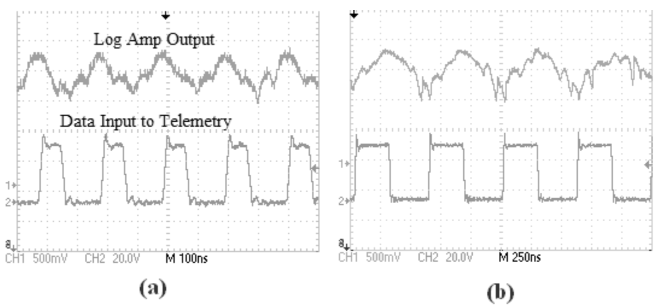

Figure 6. Demonstration of ASK transmission and demodulation. The top traces are the outputs of the logarithmic amplifier, which is part of the ASK demodulator. The bottom traces are the data inputs to the implant circuitry for reverse telemetry. (a) Telemetry at 10Mbps with a coil separation of 5mm (b) Telemetry at 3.25Mbps with a coil separation of 1cm.

In simulation, the PLL power consumption was below 1.3mW for frequencies below 100MHz with a 3V supply. The power consumption of the complete chip was measured to be 4.2mW operating at 48MHz with a 2.7V supply which is close to the simulated value of the complete chip power consumption at 48MHz, 3.7mW. According to simulation, at this frequency and power supply voltage the PLL only consumes 14% of the total power, while the reverse telemetry driver consumes 74% of the total power. The reverse telemetry driver circuitry included on the chip is not optimized for low power because it has redundant modulation and driver circuitry that was used for evaluation purposes. A more complete description of the circuitry and its measured performance, which space does not allow including here, is given in [6]. The specific contribution of this paper is the description of methods to reduce and mitigate interference of the power link upon the outward data transmission link, including the use of a differential external data coil configuration, and filtering of the class E tank circuit.

VII. Discussion

Reverse telemetry at 10Mbps and 3.25Mbps (Alternating ‘1’s and ‘0’s) is shown in Fig. 6. For this demonstration the separation between the external and implant coils was 5mm for 10Mbps transmission and 1cm for 3.25Mbps transmission. The diameter of the implant power coil was 1cm and the diameter of the implant reverse telemetry coil was 8mm, and no bypass capacitance was required for reliable operation other than the 0.66nF of on-chip bypass capacitance.

The range of reliable reverse telemetry, is limited by the fact that the wireless transmission is achieved by inductive coupling which falls off steeply with reverse telemetry coil separation. The range of reliable reverse telemetry is also limited by the noise floor which is established by switching noise from the class E transmitter, and can be improved by using a higher Q notch filter to remove harmonics from the AC current sustained in the external power coil by the class E converter. The range of reverse telemetry can also be increased if the data coil can be located outside of the power coil at the expense of implant size. This arrangement would increase the effective coupling between the data coils and potentially reduce the harmonic coupling to the external differential data coil which remains due to electrostatic effects.

VIII. Conclusion

We believe the method presented is suitable for providing 2-way communication and wireless power for a wideband neural recording system. An important aspect of the dual link design presented was the use of techniques to reduce the influence of the power link upon the data link. This paper demonstrates the utility of a differential external receiver coil and filtering of the class E tank circuit to reduce the interference introduced by harmonics distortion of current in the external power coil.

References

[1] U.M. Jow, M. Ghovanloo, “Optimization of Data Coils in a Multiband Wireless Link for Neuroprosthetic Implantable Devices,” *IEEE Transactions on Biomedical Circuits and Systems*, vol. 4, no. 5, pp. 301-310, Oct., 2010.

[2] G.Wang, W. Liu, M. Sivaprakasam, M. Zhou, J. Weiland, M. Humayun, “A Dual Band Wireless Power and Data Telemetry for Retinal Prosthesis,” *Proceedings of the28th IEEE EMBS Annual International Conference* , pp. 4392-4395, Aug. 2006.

[3] M. Zhou, W. Liu, G. Wang, M. Sivaprakasam, J. Weiland, M. Humayun, “A Transcutaneous Data Telemetry System Tolerant to Power Telemetry Interference,” *Proceedings of the28th IEEE EMBS Annual International Conference* , pp. 5884-5887, Aug. 2006.

[4] E.B. Rosa, "No 169 – Formulas and Tables for the Calculation of Mutual and Self Inductance," Scientific Papers of the Bureau of Standards, 1911.

[5] J. Maneatis, “Low-Jitter Process-Independent DLL and PLL Based on Self-Biased Techniques,” *IEEE Journal of Solid-State Circuits*, vol. 31, no. 11, pp. 1723-1732, Nov. 1996.

[6] A. Rush, P.R. Troyk, “Power and Data for a Wireless Implanted Neural Recording System, ” *Proceedings of the 5th International IEEE/EMBS Conference on Neural Engineering*, Apr. 2011.